AIP | Journal of Applied Physics

Field emission in ordered arrays of ZnO nanowires prepared by nanosphere lithography and extended Fowler-Nordheim analyses

E. McCarthy, S. Garry, D. Byrne, E. McGlynn, and J.-P. Mosnier

Related Articles

Hybrid thermal-field emission of ZnO nanowires
Appl. Phys. Lett. 99, 243108 (2011)

Screened field enhancement factor for the floating sphere model of a carbon nanotube array
J. Appl. Phys. 110, 114311 (2011)

Field-emission-assisted approach to dry micro-electro-discharge machining of carbon-nanotube forests
J. Appl. Phys. 110, 103305 (2011)

The hysteresis phenomenon of the field emission from the graphene film
Appl. Phys. Lett. 99, 173104 (2011)

Temperature dependence of the field emission from the few-layer graphene film
Appl. Phys. Lett. 99, 163103 (2011)

Additional information on J. Appl. Phys.

Journal Homepage: http://jap.aip.org/

Journal Information: http://jap.aip.org/about/about_the_journal

Top downloads: http://jap.aip.org/features/most_downloaded

Information for Authors: http://jap.aip.org/authors

Field emission in ordered arrays of ZnO nanowires prepared by nanosphere lithography and extended Fowler-Nordheim analyses

E. McCarthy,[a] S. Garry, D. Byrne, E. McGlynn, and J.-P. Mosnier

School of Physical Sciences and National Centre for Plasma Science and Technology, Dublin City University, Glasnevin, Dublin 9, Ireland

A multistage chemical method based on nanosphere lithography was used to produce hexagonally patterned arrays of ZnO vertical nanowires, with 1 μm interspacing and aspect ratio $\sim$20, with a view to study the effects of emitter uniformity on the current emitted upon application of a dc voltage across a 250 μm vacuum gap. A new treatment, based on the use of analytical expressions for the image-potential correction functions, was applied to the linear region below 2000 V of the Fowler-Nordheim (FN) plot and showed the most suitable value of the work function ϕ in the range 3.3–4.5 eV (conduction band emission) with a Schottky lowering parameter y$\sim$0.72 and a field enhancement factor γ in the 700–1100 range. A modeled γ value of $\sim$200 was calculated for an emitter shape of a prolate ellipsoid of revolution and also including the effect of nanowire screening, in fair agreement with the experimental value. The Fowler-Nordheim current densities and effective emission areas were derived as 10^{11} Am^{-2} and 10^{-17} m^2, respectively, showing that field emission likely takes place in an area of atomic dimensions at the tip of the emitter. Possible causes for the observed departure from linear FN plot behavior above 2000 V were discussed. © *2011 American Institute of Physics*. [doi:10.1063/1.3671402]

I. INTRODUCTION

There is currently much interest in the development of field emission (FE) electron sources for use in new technologies, such as flexible displays[1] or small x-ray sources.[2,3] The wide bandgap material zinc oxide has received particular attention for this application, due to its ease of nanostructure growth in a variety of possible morphologies, and favorable electronic properties such as ease of n-type doping. These properties are directly related to the key factors controlling the field-emitted current, the applied surface electric field strength F_S and the work function ϕ, respectively; as they are the fundamental parameters entering the theory developed by Fowler and Nordheim (FN) to interpret current I versus voltage V data.[4] The field emission behavior of a single, sharp, metallic emitter has been studied and analyzed using FN theory for several decades, e.g., Refs. 5–7, to include a single carbon nanotube in recent work.[8] Microelectronics devices composed of 2D-arrays of molybdenum emitting tips were also successfully developed by Spindt *et al*.[9] Significantly, these authors showed that the emission takes place in an effective, atomic-sized area of the order of 10^{-19} m^2 per tip.

The recent developments in nanotechnology fabrication methods have driven an intensive effort in the use of high aspect ratio ZnO nanostructures in field emission research due to advantageous physical and material properties.[10] Recent works typically study disordered assemblies of vertically oriented, parallel nanowires or nanorods with typical occupation density of 10^7 cm^{-2}, radii in the range 50–100 nm, heights in the range of 0.5–2 μm and overall sample surface areas of up to several cm^2.[3] The authors generally report close to linear plots obtained via standard FN analyses, assuming a uniform field in the voltage gap (V/d). They report on the field enhancement factor, the turn-on field, and the threshold field, with typical values of several thousands, 1 V μm^{-1}, and 10 V μm^{-1}, respectively.[11–15] The apparent reported scatter of field parameters and field enhancement values out of these many studies indicate no clear trends for the understanding of the effects of ZnO nanowire topology and individual morphology on the field parameters. This may be a result in part of the lack of sample uniformity on the substrate, resulting in non-uniform electric field and emission patterns, respectively.

Peculiar emission behavior has also been reported recently by several authors. Xiao *et al*.[16] have observed an unstable oscillating behavior of the $I-V$ data from single, cone-shaped ("agavelike") ZnO nanostructures, which they attribute to the combined effect of surface charging and surface atom diffusion on the nanostructure tip. Semet *et al*.[17] have reported linear FN plots for vertically aligned ZnO nanowire planar cathodes, but showed that the corresponding slopes could only be interpreted if an effective barrier height of about 1 eV was assumed that would result from structural changes at the nanowire tip due to temperature effects. We recall here that most reports on the topic of FE assume the work function value $\phi = 5.3$ eV for ZnO, irrespective of its morphology.[18] Al-Tabbakh *et al*. have recorded $I-V$ data leading to highly non-linear FN plots for ZnO tetrapod nanostructures,[19] which they interpreted in terms of conduction band electrons or valence band currents at high field values due to the saturation of the conduction band current. It is apparent that the authors invoke differing electronic processes and work function values to explain the different results observed.

---

a)Author to whom correspondence should be addressed. Electronic mail: eanna.mccarthy7@mail.dcu.ie.

In this work, we address the aforementioned issues, first, by the study of the field emission behavior of hexagonally patterned arrays of vertically aligned ZnO nanowires. This increased control over emitter topology should allow the determination of more valid field parameters. Secondly, we extend the method of the FN plot by using analytical expressions[20] for some required mathematical functions, together with plausible values of ϕ obtained from physical considerations. This provides for a general treatment of emission data within the physical framework of FN theory. The field enhancement factors computed by this treatment are compared with theoretical or modeling estimates, relating them to relevant geometrical parameters such as aspect ratio and surface density.[21–23] Effective emission areas and current densities are also calculated from the present treatment and compared with older approaches.[9,24,25] General conclusions regarding the interpretation of FE data from random or ordered arrays of ZnO nanostructures are drawn.

II. EXPERIMENTAL DETAILS

A. NSL growth

Ordered, spaced arrays of zinc oxide nanowires were produced according to the following prescription. First, a zinc oxide seed layer was chemically deposited by dropping a 0.005M solution of zinc acetate in ethanol on to a silicon substrate. This was left for 20 s, then rinsed with pure ethanol and repeated five times. The substrate was subsequently annealed at 350 °C for 20 min. The ZnO seed layer was then grown by chemical bath deposition (CBD) at 90 °C for 1 h, in a solution of 0.025M zinc nitrate dissolved in hexamine. This growth was repeated with fresh solution, giving a total growth time of 2 h. This ZnO layer was then coated with a self-assembled monolayer of 1 μm diameter polystyrene nanospheres, using the water transfer method, and allowed to dry.[26] The resulting sample was annealed at 110 °C for 40 s. An acid catalyzed silica sol, of 0.5 ml tetraethyl orthosilicate and 0.5 ml hydrochloric acid in 20 ml of ethanol, was deposited into the interstitial spaces left exposed by the close-packed nanosphere pattern. The latter was then removed by ultra-sonication in toluene first, followed by acetone. The remaining hexagonal silica surface lattice was densified by annealing at 400 °C with a 10 °C min^{-1} ramp rate. This was finally used as the substrate to deposit the ZnO nanowire arrays by vapor phase transport (VPT), with carbothermal reduction of ZnO powders and graphite as the Zn vapor source, at 900 °C for 60 min, yielding the final sample to be used in the FE measurements. Full details of the growth methods may be found in Refs. 27 and 28.

B. FE apparatus and measurements

Field emission properties (I–V) were obtained in a system with a parallel-plate electrode configuration, in a vacuum chamber with a base pressure of $\sim 10^{-8}$ mbar. The sample was positioned at a fixed distance of $d = 250 \pm 10$ μm from the flat circular face (8 mm diameter) of a stainless steel anode. This electrode assembly was mounted in series with a current-limiting resistance of

$\sim$231 kΩ. The anode dc voltage was swept between 50 V and 2500 V in steps of 1 V at a rate of 1 V s^{-1} using a programmable high voltage source (Stanford PS350). The resulting current was measured at each step through a Keithley 6485 picoammeter connected to ground.

We found in all cases these I–V measurements to exhibit hysteresis; the values of the current differ markedly when measured in increasing or decreasing voltage steps. This effect has been reported in several previous reports of FE from ZnO and in some cases leads to nonlinear FN plots,[29–31] the interpretation of which is quite uncertain as a result. This hysteresis effect is generally attributed to the effect of adsorbates, and disappears following adequate conditioning of the samples. In our case, conditioning was carried out by repeating I–V measurements in a cyclical manner until hysteresis effects could not be discerned (i.e., the difference in current on the upward and downward sweeps was less than the data scatter during a single sweep). Typically, conditioning is achieved after 150 cycles.

C. Characterization

Sample morphology was characterized by scanning electron microscopy (SEM; Karl-Zeiss EVO series) and field emission SEM (FE-SEM; Hitachi 5500).

III. RESULTS

A. SEM results

SEM images of the ZnO nanostructures are presented in Fig. 1. Figures 1(a), 1(b), and 1(c) are shown in plane view and at 60° with respect to the substrate surface. Figures 1(b) and 1(c) were obtained with a higher resolution FE-SEM and after FE conditioning and measurements.

Figure 1(a) shows a clear pattern of vertical ZnO nanowires, regularly spaced by a distance of 1 μm and positioned at the nodes of a 2D hexagonal close-packed lattice. It is apparent that there are a number of void sites which are counted from the analyses of many areas of the sample at about 10 sites per 100 μm^2. Thus, the average site surface density is of the order of 0.9 per μm^2. As the
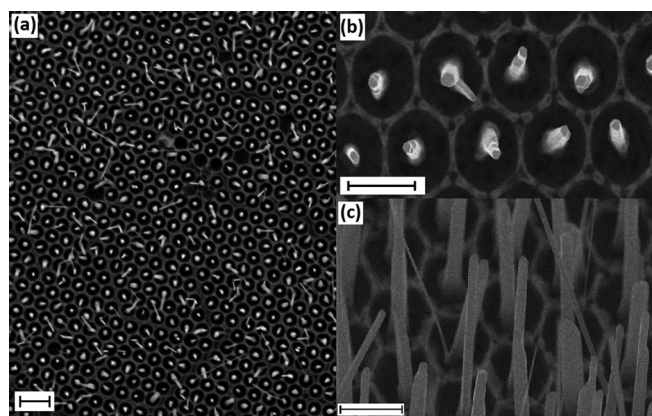

FIG. 1. SEM and FE-SEM images of ZnO nanowire array, (a) SEM of sample viewed normal to surface, (b) FE-SEM of sample viewed at 60° to the surface, (c) FE-SEM of sample viewed at 50° to the surface, with scale bars representing 2 μm, 1 μm, and 1 μm, respectively.

electrode assembly covers an area of 5×10^{-5} m^2, a total of $\sim 4.5 \times 10^7$ nodes (nanowires) is sampled in a FE measurement.

From Figs. 1(b) and 1(c), we observe that the typical morphology of a single nanowire is the familiar hexagonal prism oriented along the $\langle 002 \rangle$ direction; of average height around 2 μm, with a standard deviation of ~ 0.29 μm; and average largest width/diameter of 0.2 μm, with a standard deviation of ~ 58 nm (aspect ratio of ~ 20). The ratio of inter-nanowire distance to nanowire length is therefore equal to 0.5. The nanowire dimensions imply a cross-sectional area of 2.6×10^{-2} μm^2 (or 3.1×10^{-2} μm^2 if a circular cross-section is assumed). This is close to the values of this ratio suggested in the literature as suitable for optimized FE.[32] The tip shape of the majority of the nanowires is curved outward rather than sharply pointed, and rarely seen to be flat-ended. We note from Figs. 1(b) and 1(c) that the processes of conditioning and field emission do not appear to have a pronounced effect on the observable nanowire morphology. In particular, the change to a bulbous morphology at the tip, driven by temperature-dependent surface migration as featured in the Ref. 17, is virtually absent from the present data. X-ray diffraction data (not shown) have confirmed these observations, showing very intense (002) diffraction peaks at 34.3°. However, we are unable to determine from experiment whether the nanowires are either positively (0001) zinc- or negatively (000-1) oxygen-terminated or if a mixture of the two possible terminations prevails. Many other authors have reported, however, that the (0001) zinc-terminated face tends to appear more tapered and this is consistent with the morphology we observe.

B. I–V graphs

The final reproducible I–V data (total of 4900 data points) obtained after the many conditioning cycles is displayed in the main part of Fig. 2. In the inset, we show an extended FN plot of $\log_{10} I/V^2$ vs $1/V$ for all the points, showing the turn-on voltage of ~ 1000 V which we define as

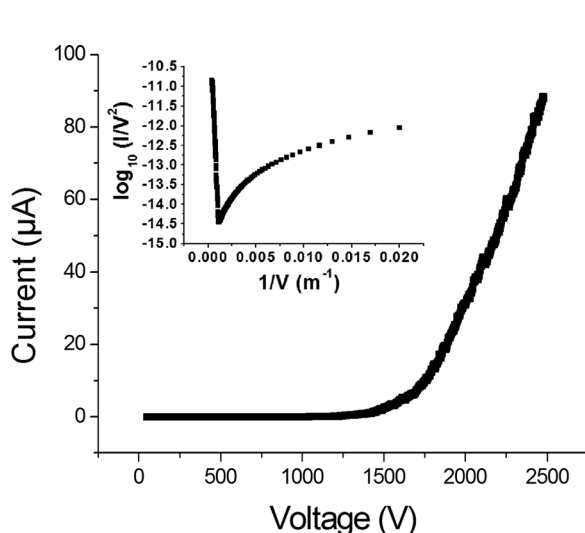the voltage above which the FN plot shows good linear behavior. We measure typical currents of the order of ~ 2.0 μA to ~ 90 μA between 1500 V and 2500 V. Above the latter voltage, frequent arcing prevents continuous measurements, which may indicate the limit of field emission (see discussion in Sec. IV). Therefore, the range of voltages usable for FE measurements appears quite narrow, as mentioned previously.[5]

IV. ANALYSES

A. FN plots

All the experimental data above the turn-on voltage are converted to a FN plot and displayed in Fig. 3 as $\log_{10} I/V^2$ vs $1/V$ (bottom x scale and left y scale) and $\log_e I/F_m^2$ vs $1/F_m$ (top x scale and right y scale), where F_m is the applied field defined as $F_m = V/d$ with $d = (250 \pm 10) \mu$m. As a result of the large number of data points, we have run a numerical 5-point average to smooth the curve and, thus, make deviations from linear behavior more apparent. As a result, we clearly distinguish two linear domains in the graph, corresponding to regions of low and high voltages, below and above 2000 V, respectively. The curve is linear in these two domains, as shown in Fig. 3, with a significant change in the observed slope (the apparent small deviations from linearity observed in the very low voltage region are not considered to be physically significant, and are mostly like noise due to stray fields and/or leakage currents). The observed behavior is typical of electron field emission with the distinct change in slope in the high voltage region generally attributed to the buildup of a significant amount of space-charge.[14,33]

In the present paper, we shall use the equations describing cold FN emission expressed in their basic forms under the physical assumptions of their applicability.[6] The slope values of the two linear regimes observed in the $\log_{10} I/V^2$ vs $1/V$ graph are measured at -5745 V and -2702 V, respectively.

FIG. 2. Current vs voltage plot, inset shows a FN plot covering the full data range.
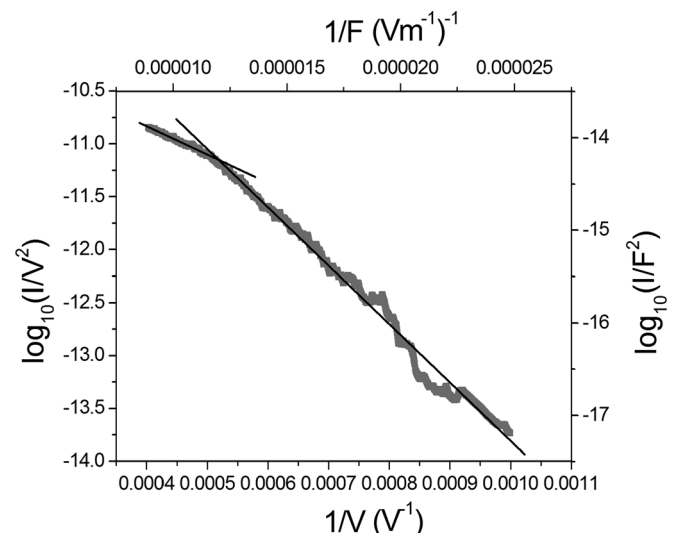

FIG. 3. FN plots: $\log_{10}(I/V^2)$ vs $1/V$ and $\log_{10}(I/F^2)$ vs $1/F$, with lines denoting two distinct linear regions.

TABLE I. Work function, electron affinity, and band bending for the hexagonal faces of ZnO.

Reference	Work function ϕ (eV)		Electron affinity χ (eV)		Band bending ($\pm$eV) upward (+), downward (−)	
	(0001)Zn	(000-1)O	(0001)Zn	(000-1)O	(0001)Zn	(0001)O
Ref. 30 clean, annealed surfaces	3.7	6.0	3.7	4.5	−0.2	1.3
Ref. 30 reconstructed, adsorbed	3.3	4.3	3.3	3.9	−0.2	0.15
Ref. 31	3.15	4.85	3.35	5.05	< −0.3	
Ref. 35			4.1			
Ref. 18 polycrystalline thin film	5.3	5.3				

B. Work function

It is established that the slope of a FN plot is mainly determined by the value of the work function ϕ.[34] In order to interpret our data with the minimum number of *a priori* assumptions, we have surveyed the literature to find what possible values of ϕ should be used in the case of ZnO. The data are summarized in Table I. Jacobi *et al.* have carried out detailed angle-resolved ultraviolet photoelectron spectroscopy (UPS) measurements on clean, annealed ZnO polar (0001) and (000-1) faces[30] and measured the corresponding values of the work function, electron affinity, and band bending. These were found to rapidly change as a function of time due to surface reconstruction, defect creation, and gas adsorption effects and reach asymptotic values of 3.3 eV and 4.3 eV, respectively. We believe that these asymptotic values should be used for the ZnO material in the present work, which has been exposed to ambient conditions for extended periods. Marien[31] has measured the work function of the polar faces of ZnO needles using a combination of FN characteristics and low-field ionization characteristics, independently of any possible field enhancement factors. The Fermi level is placed 0.2 eV below the conduction band minimum in the bulk in these works. A value of 4.1 eV is quoted in Ref. 35 for the electron affinity of the (0001) face, based on Schottky contact barrier measurements. Semet *et al.*[17] accounted satisfactorily for their experimental observations on ⟨002⟩ vertically aligned ZnO nanowires if they assume an actual work function of the order of 1 eV due to severe modification of the electronic and structural properties of the emitting surface after prolonged field emission. Finally, we note that a value of 5.3 eV is very commonly used by authors working in the ZnO nanowire FE field and obtained by Minami *et al.* for magnetron-sputtered ZnO thin films.[36] On the basis of the above review, we believe that the work function value of 5.3 eV is possibly more appropriate for ZnO polycrystalline material or disordered nanowire assemblies.

C. Slopes and enhancement factors

All the formulae presented here are expressed in SI units. The slope of the FN $\log_{10}(I/V^2)$ vs $1/V$ plot can be written as $m = -2.97 \times 10^9 \frac{\phi^{3/2} s(y)}{2.3\beta}$, where β is a geometrical factor in m^{-1} determined by the local and large-scale geometries of the electrode assembly and such that $F_S = \beta V$, where F_S is the field strength at the surface. This means that the β value obtained for an array of emitters represents the single tip current weighted average taken over the tip surface and the entire array.[22] $s(y)$ is a tabulated function of the variable $y = 3.79 \times 10^{-5} \frac{F_s^{1/2}}{\phi} = 3.79 \times 10^{-5} \frac{(\beta V)^{1/2}}{\phi}$, which represents the Schottky lowering of the work function barrier. Forbes has shown that $s(y)$ can be accurately evaluated using the following analytical expression $s(y) = 1 - \frac{1}{6}y^2$.[20] At very low applied field, the image force correction is negligible, and $s(y) \approx 1$.[3] If one fixes the value for the work function, then β can be evaluated using successive approximations based on the above equations. The measured slope is used to calculate a value for β assuming $s(y) \approx 1$. This allows the calculation of a value for y, which in turns allows the calculation of the value of $s(y)$. This procedure is repeated until convergence, which typically takes no more than five iterations. We have carried out such calculations for the various values of ϕ as discussed in Sec. IV B at the moderate voltage value of 1500 V. The results are presented in Table II. The Nordheim functions $v(y)$ and $t(y)$ are also evaluated using the analytical expressions given in Ref. 20. We also provide the value of the field enhancement factor γ defined by $\gamma = F_S/F_m = \beta d$. The current density can thus be calculated using the FN equation

$$J = 1.54 \times 10^{-6} \frac{F_S^2}{\phi t^2(y)} \exp\left(-\frac{6.834 \times 10^9 \phi^{\frac{3}{2}}}{F_S} v(y)\right) \text{in Am}^{-2}.$$

TABLE II. Calculated Fowler-Nordheim parameters for various possible values of the work function.

Work function ϕ (eV)	y	β (m^{-1})	$\gamma = \beta d$	$s(y)$	$v(y)$	$t(y)$	F_S (Vm^{-1})	J_{FN} (Am^{-2})	$A_{FN} = \frac{2.45 \times 10^{-6}}{J}$ (m^2)
1.0	0.97	0.4×10^6	109	0.84	0.05	1.11	7×10^8	3.2×10^{11}	7.7×10^{-18}
3.3	0.74	2.8×10^6	703	0.91	0.39	1.08	42×10^8	1.6×10^{11}	1.5×10^{-17}
3.7	0.73	3.4×10^6	839	0.91	0.42	1.08	50×10^8	1.6×10^{11}	1.5×10^{-17}
4.5	0.70	4.5×10^6	1135	0.92	0.46	1.07	68×10^8	1.7×10^{11}	1.4×10^{-17}
5.3	0.67	5.8×10^6	1460	0.93	0.49	1.07	88×10^8	1.8×10^{11}	1.4×10^{-17}
7.9	0.61	10.8×10^6	2693	0.94	0.57	1.06	162×10^8	3.2×10^{11}	1.1×10^{-17}

From Table II, we observe typical surface field and current density values of $\sim 10^9$ Vm^{-1} and $\sim 10^{11}$ Am^{-2}, respectively. These are compatible with the results of similar types of FN analyses of sharp emitters.[9] We note that the use of a work function of 1.0 eV corresponds to a case of almost complete lowering of the barrier ($y \approx 1$) and, thus,would appear unsuitable for further interpretation of our data. For $3.3 \leq \phi \leq 4.5$ eV, corresponding to conduction band electrons in the flatband diagram, the lowering of the barrier is moderate ($y \approx 0.7$) and does not exceed the physical limit $y = 1$ at $V = 2500$ V, suggesting that the emission process is compatible with FN field emission. In this work function range, the field enhancement values (700–1100) are markedly lower than those reported in Refs. 11, 14, 15, and 33 based on the 5.3 eV value. The choice of a work function of $\phi = 7.9$ eV corresponding to electrons emitted from the top of the ZnO valence band[19] leads to even larger values of the enhancement factor and the surface field strength.

The field strength at the surface is related to the voltage difference between the electrodes via a factor that depends both on the geometry of an individual nanowire emitter and the nanowire spatial distribution on the cathode surface. We now compare our experimental values with calculated values obtained from various theoretical models expressing the enhancement at the apex of the nanostructure γ_a. Forbes *et al.*[23] have summarized a number of models and approximations for γ_a in terms of the ratio of the total protrusion length to the base radius of a single emitter, which we approximate to the aspect ratio of height to half-width in our case (~ 20). From Table I of Ref. 23, we obtain γ_a values ranging from 15 to 450 for hemisphere-on-post to hemi-ellipsoid (with an apex radius of curvature $r_a \sim 5$ nm) models, respectively. The hemi-ellipsoid model of Kirkpatrick *et al.*[21] gives a similar value of ~ 145. Read and Bowring[22] and references therein, do take account of the influence of electrostatic shielding explicitly on γ_a for a specific type of array of emitters specified by its surface density in a square array topology. This depends on the individual nanowire aspect ratio (~ 20) and the ratio of the inter-rod spacing to rod height (0.5) and is written in the form of a correction factor to the individual enhancement factor. This correction factor as calculated from the Read and Bowring formula[22] is 0.43, thereby reducing all previous individual γ_a by roughly 50%, which now range between 7 and 195 for hemisphere-on-post to hemi-ellipsoid models, respectively. When comparing these values with those of Table II, we observe a generally poor agreement, with discrepancies by factors of between 5 and 8. Similar disagreement levels between measurements and calculations are also common in the current literature on the topic of ZnO nanowire FE.[15,17,33]

We observe that the hemi-ellipsoid model provides the nearest agreement here, although the resolution of the microscopy used did not allow us to make a quantitative comparison. We note, however, that the HRTEM images of the extreme tip of ZnO nanowires shown in Ref. 14 appear to support this shape. We note that nanowire parameter values of $r_a \sim 2.5$ nm requiring a base radius of 70 nm for

the same 2 μm length would yield a value of ~ 840 for γ_a. Notwithstanding the effects of the array screening, these values, which are feasible for this type of structure, would bring the calculated and measured enhancement factors into good agreement. We recall that this value of γ_a is obtained for a work function $\phi = 3.7$ eV and note that using the common value of $\phi = 5.3$ eV has the effect of increasing this disagreement. We suggest that more work is required to justify more strongly the use of the numerical value of $\phi = 5.3$ eV for the work function of ZnO nanowires within the framework of FN theory.

We also note that the field enhancement factors reported here, and commonly by other authors, are based on the use of the β-modified FN theory, which would not generally apply to nanometric-sized emitters.[37,38] The importance of these small size-effects can be estimated by comparing the ratio of the width of the barrier at the Fermi level to a characteristic curvature of the nano-emitter. We calculate this ratio for $V = 1500$ V and $\phi = 3.7$ eV to be 6 or 120 for an emitter characteristic curvature of 100 nm or 5 nm, respectively. As these are significantly greater than 1, we conclude that the use of a modified FN theory is probably required in the present case to interpret the experimental data correctly, and more generally, this could also be said about any FE experiment on ZnO nanowires of similar sizes to the ones used here.

We have pointed out the two linear regimes observed in the FN plot of Fig. 3. The slope value in the high-field regime is measured at -2702 V and is significantly reduced compared with its value in the low field regime. We observe that the transition between these regimes occurs gradually around a voltage of 2 kV over a range of about 150 V. We note that these two distinct regimes are also observed by Jeong *et al.*[14] in the case of ZnO nanowires and Al-Tabbakh *et al.*[19] in the ZnO tetrapods.

Such high-field deviations from the FN straight-line have been commonly observed in FE experiments and typically interpreted in terms of the occurrence of space-charge effects at higher currents.[4,36,37] A basic numerical criterion for neglecting space-charge effects, according to which the parameter $T \ll 1$, is presented in Refs. 4 and 39. We calculate T to be equal to ~ 0.06 and ~ 0.4 at 1500 V and 2000 V, respectively, showing that space-charge effects are probably contributing to the observed current behavior in our high-field region.

Besides space-charge effects, the lower slope of the FN plots at high field, within the framework of cold emission FN theory, can be due to two effects: changes in the work function[40] or the field enhancement factor.[21] As a larger surface area of the emitter will contribute to the emission at higher fields, the assumption of a non-uniform work function over the probe area is reasonable. Also, contributing tips having different crystallographic terminations may have a contribution and we have shown previously in this section that a small change in the value of the work function can significantly alter the outcome of the FN analysis. The work functions of other faces of ZnO have been measured: 5.05 eV for the prismatic faces[30] and 4.05 eV for the (10-1-1) faces,[31] and show sufficient variance to have an effect if engaged in

the field emission process. Kirkpatrick *et al.*[21] have shown that for an emitter with nanometric-sized tips of hemi-ellipsoidal shape the field enhancement factor γ decreases and the effective emission area α increases with increasing applied field, while a standard FN analysis would lead to the opposite conclusion (see also Ref. [37]). This is supported by our high-field data that an increased γ value of 1540 would be obtained at 2000 V if a constant work function of 3.7 eV were assumed. Furthermore, this analysis would yield a $y > 1$, indicating an inconsistency in the FN plot analysis. We have shown that the departure from FN linearity at high field can be satisfactorily accounted for by the field dependence of the work function and the enhancement factor. Alternative explanations, based on the semiconductor electronic structure of ZnO, have been put forward by other authors. Jeong *et al.*[14] suggested that the emission proceeds from deep-level defect states in the low field regime whereas the high field regime consists of electrons emitted from near the Fermi level. Al-Tabbakh *et al.*[19] suggested that low-field emission in the conduction band ultimately saturates as the field is increased and leads to predominant emission from the valence band in the high field regime with a related increase in the work function value. More detailed investigations are needed to understand the importance of semiconductor effects in the FE of ZnO nanowires. For example, the emission current behavior as a function of n-type dopant concentration would be interesting in this regard.

D. Effective emission areas and current densities

From an $I-V$ measurement, one can estimate a value for the emission area A when the current density J is obtained, via $A = I/J$. In the case of a large-area electron source composed of many identical sharp emitters, this area is an average over the tip surface weighted by the local value of the current density and extended to the macroscopic area of the sample.[4,14,41] We now extract values for this emission area, denoted here as A_{FN}, from our measured data using various approaches.

First, we compute values of A_{FN} from the data of Table II and these values are listed in the far right-hand column of Table II. The values were obtained for $I = 2.45$ μA and $V = 1500$ V. We observe, as expected, that the values of A_{FN} are small compared to the surface area of the tip of one nanowire that would be obtained from its estimated dimensions (see Sec. II) and weakly dependent on the value of the work function in the 3.0–8.0 eV range. Secondly, we compute values for A_{FN} based on the approaches described in detail in Refs. [9] and [24] and described as the "effective emitting area" therein and as the "notional emission area A_n" in Ref. [41]. These authors have found equations relating the FN current density to the slope m of the FN plot,[24] or of the I–V plot,[9] which depend very weakly on the value of the work function if it is in the range 3.5 eV $\leq \phi \leq$ 11.5 eV and based on the use of a quadratic approximation for the $v(y)$ function and constant values for the $s(y)$ and $t(y)$ functions. These equations are written in terms of the variable $K = \frac{m}{V}$, which depends on E and ϕ only.[6] Improvements on the precision of the methods of Refs. [9] and [24] for the evaluation of A_{FN} have
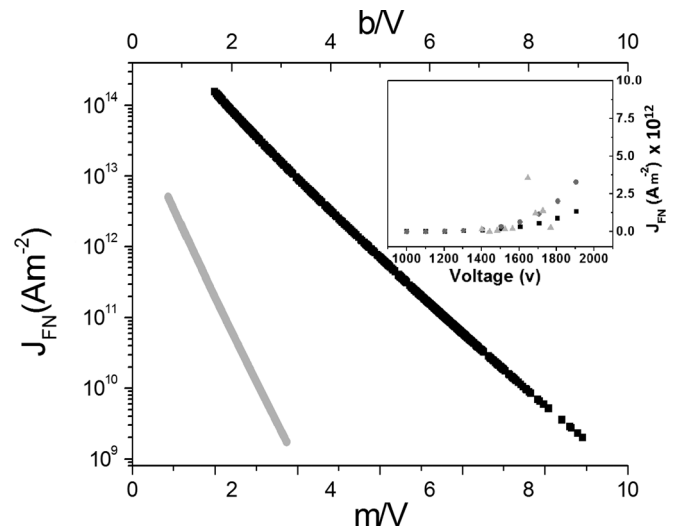

FIG. 4. Log plot of current density, J_{FN}, vs m/V in gray and J_{FN} vs b/V in black; inset shows a plot of J_{FN} vs voltage for three methods, from FN estimation in black squares, from Charbonnier's method (Ref. [24]) in dark gray circles, and from Spindt's method (Ref. [9]) in light gray triangles.

been detailed in Ref. [25] and references therein. However, these would not affect the conclusions of the present work.

The results are presented in Fig. [4] in the form of a graph of $\log_{10} J_{FN}$ vs $\frac{m}{V}$ using the approach of Ref. [24] and a graph of $\log_{10} J_{FN}$ vs $\frac{b}{V}$ where $\frac{b}{V} = \frac{V}{I}\frac{dI}{dV} - 2$, using the approach described in Ref. [9]. In the insert, we plot J_{FN} as a function of voltage V including also the values obtained directly from the computation of the FN equation, as presented in Sec. [IV A]. We observe a generally good agreement between the three methods, although the values obtained using the Spindt *et al.* approach[9] tend to be noisier. This is a result of the numerical procedure we have used in which the slope $\frac{dI}{dV}$ was obtained by polynomial fitting of the experimental data and manual differentiation. In the original work, $\frac{dI}{dV}$ was obtained experimentally.

In Fig. [5], the values of A_{FN} deduced from Fig. [4] are shown as a function of voltage V for the same three approaches. Again, we see typical values for A_{FN} of about
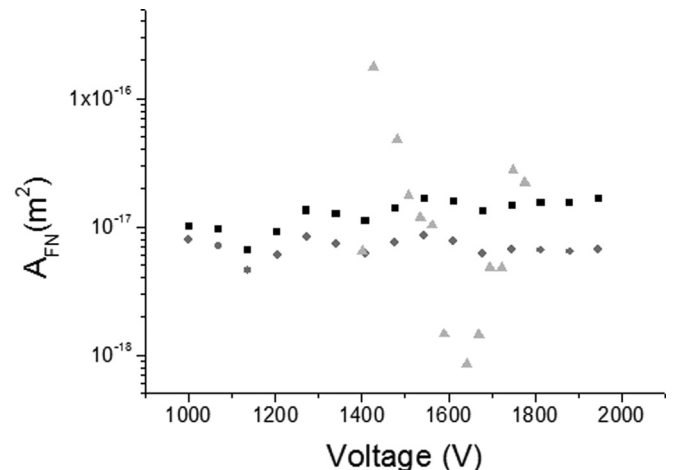

FIG. 5. Plot of area, A_{FN}, vs voltage for three methods, from FN estimation in black squares, from Charbonnier's method in dark gray circles, and from Spindt's method in light gray triangles.

1.5×10^{-17} m^2 at 1500 V with agreement within a factor of two between the three methods. From these observations, we can make the following conclusions. In view of the number of nodes ($\sim 4.5 \times 10^7$) probed by the anode in the present conditions, the effective emitting area per nanowire can only be of dimensions of the order of a few atomic sites, even if only 1% of the nanowires are actual emitters. Spindt *et al.*[9] conclude identically although we should emphasize the significant difference in the morphology, nature (metallic), and surface density of the molydnemum emitter cones used.

Finally, from the viewpoint of electronic display devices, we can compute the following figures of merit for our ZnO nanowire array cathode. The onset voltage of field emission was around 1000 V at which the device emitted a current of 14 nA, corresponding to a macroscopic current density of 2.7×10^{-3} Am^{-2} and an applied field of 4×10^6 Vm^{-1}. To obtain a threshold current of 10 mA cm^{-2} required a voltage of 1323 V, corresponding to an applied field of 5.3×10^6 Vm^{-1} with an emitted current of 513 nA. At 2000 V, the macroscopic current density is 0.62 Am^{-2}, corresponding to a current per nanowire of 31 nA (assuming 50% efficiency). Thus, we believe that these figures prove the potential of ZnO nanowire arrays for device applications such as flat-panel displays.[1]

V. CONCLUSIONS

We have investigated field emission in ordered arrays of ZnO nanowires by measuring the total current emitted by this assembly as a function of applied voltage between 50 V and 2500 V. No stable emission could be obtained above 2500 V. The current-voltage data was analyzed by constructing Fowler-Nordheim plots which clearly showed two distinct linear regimes at low and high (above 2000 V) applied voltage, respectively. In the low-voltage region, field enhancement factors were obtained from the slope of the FN plot using a new iterative method in which the slope corrective factor due to image force is computed accurately through the use of an exact analytical function. Because the value of the work function has a strong effect on the final result, a critical review of the work function suitable for c-axis oriented ZnO nanowire field emitters was also carried out. The calculation of the field enhancement factor was repeated for a number of possible work functions, and its value assessed on the basis of the corresponding value of the Schottky lowering parameter y. According to these analyses, the best values for the field enhancement factor (with an estimated relative uncertainty of 15%) were found to be between ~ 700 and ~ 1100 for values of the work function between 3.3 eV and 4.5 eV. The enhancement factors were compared with a range of calculated values predicted by a variety of models based on the emitter shape. The agreement is found to be generally poor, except for the model in which the shape of the nanowire is assumed to be a prolate ellipsoid of revolution for which an enhancement factor of ~ 450 was calculated. The effect of nanowire screening was also investigated and found to reduce the enhancement factors by a factor of ~ 0.5 in our case. On the basis of such a shape, it was found that reducing the nanowire diameter to a value of ~ 50 nm

would give reasonable agreement between the measured and calculated enhancement factor. When applying similar analyses in the high-voltage region of much reduced slope, unrealistic values were obtained for the values of y and the field enhancement factor. A number of plausible physical mechanisms were discussed to account for the observed change of slope.

The Fowler-Nordheim current densities and effective emission areas were calculated using various methods and shown to be in good agreement. These were typically of the order of 10^{11} Am^{-2} and 10^{-17} m^2, respectively. The physical model according to which field emission takes place from an area of atomic dimensions at the tip of the emitter was supported in the case of ZnO nanowires based on the data and analysis above.

Figures of merit for device application of our nanowire arrays were presented.

On the basis of the above findings, we suggest that further work should be carried out to clarify the following points. (1) The physical reasons for the observed departure from Fowler-Nordheim law at high voltages needs to be investigated with specific attention to the clarification of the energy states of the emitted electrons and also the influence of high-density surface states.[42] (2) A better understanding of the exact effect of the emitter morphology on the efficiency of field emission. This requires the availability of well-controlled and well-defined sample geometries. (3) A detailed investigation of the work function for ZnO nanowires. (4) The understanding of the difference and the relationship between the notional and effective emission areas, which could be achieved by the use of a phosphor coated, transparent anode coupled with an imaging system. Work is currently in progress in our laboratory along these lines.

[1]J. D. Carey, Phil. Trans. R. Soc. Lond. A **361**, 2891 (2003).

[2]S. G. Wang, X. Calderon, R. Peng, E. C. Schrieber, O. Zhou, and S. Chang, Appl. Phys. Lett. **98**, 213701 (2011).

[3]C. J. Lee, T. J. Lee, S. C. Lyu, Y. Zhang, H. Ruh, and H. J. Lee, Appl. Phys. Lett. **81**, 3648–3650 (2002).

[4]T. E. Stern, B. S. Gossling, and R. H. Fowler, Proc. Roy. Soc. London A **124**, 699 (1929).

[5]R. Gomer, *Field Emission and Field Ionization* (Harvard University Press, Cambridge, MA, 1961).

[6]A. G. J. Van Oostrom, Philips Res. Rep., Suppl. **1**, 1 (1966).

[7]F. Charbonnier, Appl. Surf. Sci. **94–95**, 26 (1996).

[8]J. M. Bonard, K. A. Dean, B. F. Coll, and C. Klinke, Phys. Rev. Lett. **89**, 197602 (2002).

[9]C. A. Spindt, I. Brodie, L. Humphrey, and E. R. Westerberg, J. Appl. Phys. **47**, 5248 (1976).

[10]X. D. Wang, J. Zhou, C. S. Lao, J. H. Song, N. S. Xu, and X. L. Wang, Adv. Mater. **19**, 1627 (2007).

[11]Q. Zhao, H. Z. Zhang, Y. W. Zhu, S. Q. Feng, X. C. Sun, J. Xu, and D. P. Yu, Appl. Phys. Lett. **86**, 203115 (2005).

[12]Y. H. Yang, B. Wang, N. S. Xu, and G. W. Yang, Appl. Phys. Lett. **89**, 043108 (2006).

[13]J. Singh, S. S. Patil, M. A. More, D. S. Joag, R. S. Tiwari, and O. N. Srivastava, Appl. Surf. Sci. **256**, 6157 (2010).

[14]S. J. Jong, Y. L. Jeong, and K. C. Hyung, Chem. Phys. Lett. **503**, 266 (2011).

[15]L. Yao, M. Zhang, M. La, M. Li, M. Li, and W. Z. Shen, Nanoscale Res. Lett. **6**, 74 (2011).

[16]Z. M. Xiao, J. C. She, Z. B. Li, Y. H. Yang, G. W. Yang, S. Z. Deng, and J. Chen, J. Appl. Phys. **106**, 014310 (2009).

[17]V. Semet, T. B. Vu, T. Pauporte, L. Jouland, and F. J. Vermersch, J. Appl. Phys. **109**, 054301 (2011).

[18]T. Minami, T. Miyata, and T. Yamamoto, Surf. Coat. Technol. **108–109**, 583 (1998).

[19]A. A. Al-Tabbakh, M. A. More, D. S. Joag, I. S. Mulla, and V. K. Pillai, ACS Nano **4**, 5585 (2010); see also A. A. Al-Tabbakh, M. A. More, D. S. Joag, N. S. Ramgir, I. S. Mulla, and V. K. Pillai Appl. Phys. Lett. **90**, 162102 (2007).

[20]R. G. Forbes, Appl. Phys. Lett. **89**, 113122 (2006)

[21]D. A. Kirkpatrick, A. Mankofsky, and K. T. Tsang, Appl. Phys. Lett. **60**, 2065 (1992).

[22]F. H. Read and N. J. Bowring, Nucl. Instrum. Methods A **519**, 305 (2004).

[23]R. G. Forbes, C. J. Edgcombe, and U. Valdrè, Ultramicroscopy **95**, 57 (2003).

[24]F. M. Charbonnier and E. E. Martin, J. Appl. Phys. **33**, 1897 (1962).

[25]R. G. Forbes and K. L. Jensen, Ultramicroscopy **89**, 17 (2001).

[26]S. Garry, E. McCarthy, J. P. Mosnier, and E. McGlynn, Appl. Surf. Sci. **257**, 5159 (2011).

[27]D. Byrne, E. McGlynn, J. Cullen, and M. O. Henry, Nanoscale **3**, 1675 (2011).

[28]D. Byrne, E. McGlynn, K. Kumar, M. Biswas, M. O. Henry, and G. Hughes, Cryst. Growth Des. **10**, 2400 (2010).

[29]H. Z. Zhang and R. M. Wang, J. Appl. Phys. **96**(1), 624 (2004).

[30]K. Jacobi, G. Zwicker, and A. Gutmann, Surf. Sci. **141**, 109 (1984).

[31]J. Marien, Phys. Status Solidi A **38**, 513 (1976).

[32]J. S. Suh, K. S. Jeong, J. S. Lee, and I. T. Han, Appl. Phys. Lett. **80**, 2392 (2002).

[33]R. N. Gayen, S. Dalui, A. Rajaram, and A. K. Pal, Appl. Surf. Sci **255**, 4902 (2009).

[34]R. H. Good and E. W. Muller, *Handbuch der Physik* (Springer, Berlin, 1956), Vol. 21, p. 176.

[35]C. F. Klingshirn, B. K. Meyer, A. Waag, and A. Hoffman, *Zinc Oxide From Fundamental Properties Towards Novel Applications* (Springer, Berlin, 2010).

[36]J. P. Barbour, W. W. Dolan, J. K. Trolan, E. E. Martin, and W. P. Dyke, Phys. Rev. **92**, 45 (1953).

[37]P. H. Cutler, J. He, J. Miller, N. M. Miskovsky, B. Weiss, and T. E. Sullivan, Prog. Surf. Sci. **42**, 169 (1993); P. H. Cutler, J. He, N. M. Miskovsky, T. E. Sullivan, and B. Weiss, J. Vac. Sci. Technol. B **11**, 387 (1993).

[38]T. J. Lewis, Phys. Rev. **101**, 1694 (1956).

[39]G. N. Fursey, *Field Emission in Vacuum Microelectronics* (Kluwer Academic/Plenum, New York, 2005).

[40]G. N. Fursey and D. V. Glazanov, J. Vac. Sci. Technol. B **16**, 910 (1998).

[41]R. G. Forbes, J. Vac. Sci. Technol. B **27**, 1200 (2009).

[42]N. Rihon, Phys. Status Solidi A **63**, 617 (1981).